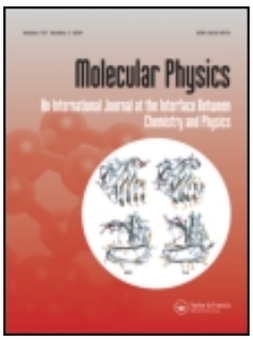

Molecular Physics

ISSN: 0026-8976 (Print) 1362-3028 (Online) Journal homepage: http://www.tandfonline.com/loi/tmph20

ENDOR investigations of the structure of glycine radicals in X-irradiated tri-glycine sulphate and of structural changes near the ferroelectric phase transition point

M. Welter , T. Kröber , S. Wartewig & W. Windsch

To cite this article: M. Welter , T. Kröber , S. Wartewig & W. Windsch (1978) ENDOR investigations of the structure of glycine radicals in X-irradiated tri-glycine sulphate and of structural changes near the ferroelectric phase transition point, Molecular Physics, 36:5, 1385-1395, DOI: 10.1080/00268977800102431

To link to this article: http://dx.doi.org/10.1080/00268977800102431

MOLECULAR PHYSICS, 1978, VOL. 36, NO. 5, 1385–1395

ENDOR investigations of the structure of glycine radicals in X-irradiated tri-glycine sulphate and of structural changes near the ferroelectric phase transition point

Part 1. The structure of glycine radicals in X-irradiated tri-glycine sulphate

by M. WELTER, T. KRÖBER, S. WARTEWIG
and W. WINDSCH

Sektion Physik der Karl-Marx-Universität,
DDR 701 Leipzig, German Democratic Republic

(*Received* 8 *December* 1977)

A report is given on ENDOR investigations of the structure of radicals in X-irradiated tri-glycine sulphate single crystals at 77 K and 300 K. Two non-equivalent radicals of the type NH_3^+–$\dot{C}H$–COO^- which originate at sites on the glycine molecules gly II and gly III were identified. Their hyperfine coupling parameters differ by a maximum of 1 MHz at room temperature. The radicals have non-equivalent β-protons indicating strongly hindered rotation of the amino group. INDO calculations were also performed. The radicals were found to be non-planar. The proton deviates from the nodal plane of the π-orbital by about 10°. The positions of the hydrogen atoms of the amino groups were found to agree with the corresponding hydrogen bonds in the non-irradiated crystals.

1. INTRODUCTION

In recent years, nuclear magnetic resonance (N.M.R.), nuclear quadrupole resonance (N.Q.R.), and electron paramagnetic resonance (E.P.R.) studies have been made on both tri-glycine sulphate (TGS) and deuteriated TGS in an effort to clarify the structures of glycine and glycinium molecules, the structures of radicals of these molecules that result from irradiation of the crystals, and the structural changes caused by the ferroelectric phase transition. Whereas N.M.R. investigations provide valuable information about the nature of the phase transition [1], the reorientation of certain groups [2], and the dynamics of the phase transition [3], E.P.R. studies of γ-ray and X-ray irradiated crystals have not been very successful so far. Initial E.P.R. studies made on γ-ray irradiated single crystals and powders of TGS, by Ovenall and Müller [4], Blinc *et al.* [5], and Schulga [6] provide evidence for the existence of NH_3^+–$\dot{C}H$–COO^- type radicals. However, no change in the structure of this radical was observed during the ferroelectric phase transition. Kato and Abe [7] later discovered an additional $\dot{C}H_2$–COO^- type of radical whose dynamics are of great interest but which has no relation to the ferroelectric phase transition.

Clear evidence of a change in structure due to the ferroelectric phase transition was first obtained by Kato and Abe [8] for the NH_3^+–$\dot{C}H$–COO^- radical

with a rapidly rotating amino group. They showed that the hyperfine coupling tensors for the β-protons of glycine II and III differ only slightly in the ferroelectric phase and that this non-equivalence steadily disappears as the Curie temperature is approached.

The electron nuclear double resonance (ENDOR) technique used by the authors for analysing the structures of NH_3^+–$\dot{C}H$–COO^- type radicals in irradiated TGS makes it possible to detect not only centres with a rapidly rotating amino group, but also those centres whose amino groups rotate at frequencies less than about 10^5 Hz, and to determine accurately the structure of the resulting hydrogen bridge system.

The results of our ENDOR studies indicate that irradiation has no adverse effect on the hydrogen bridge system. Consequently, they permit accurate determination of the spatial and electronic structures in the paraelectric and ferroelectric phases. INDO calculations were carried out to confirm ideas relating to the structures of the two radicals in TGS deduced from ENDOR experiments.

The structural changes of this radical observed in the vicinity of the phase transition temperature and notions concerning the possible mechanism of ferroelectric phase transition will be discussed in part 2 of this paper.

2. Crystal structure of TGS

Hoshino *et al.* [9] have shown that TGS, in the ferroelectric phase, has a monoclinic crystal lattice with the following parameters: $a = 9{\cdot}41_7$ Å; $b = 12{\cdot}64_3$ Å; $c = 5{\cdot}73_5$ Å; $\beta = 110° 23'$. The space group is $P2_1$, and the polar axis lies in the direction of the twofold screw axis (b-axis). The chemical formula is $(NH_3^+CH_2COO^-)(NH_3^+CH_2COOH)_2SO_4^{2-}$. The unit cell contains two chemical units. More recent structural studies have been made by Itoh and Mitsui [10] and by Kay and Kleinberg [11].

3. Experimental

3.1. *Preparation of samples and dielectric studies*

Crystals were grown in an aqueous solution by slow evaporation at about 35°C, using the method of Nitsche [12]. Irradiation was from a 20 kV, 20 mA X-ray source. The time of irradiation was two hours, and the concentration of centres obtained was of the order of 10^{18} cm^{-3}. Crystals used for studying the temperature dependence of hyperfine tensors were carefully cut to enable rotation about the principal axes of the tensors, the directions of which were determined at 25°C. Adjustment of crystals was performed in the cavity of the ENDOR spectrometer with an accuracy of better than 1°.

In order to characterize the dielectric properties of the samples used in these studies, the temperature dependence of the dielectric constant, ϵ_b, for differently irradiated samples was monitored at a measuring frequency of 100 kHz. The maximum value of the dielectric constant decreases as the time of irradiation increases and the Curie–Weiss temperature, which is almost identical in this case with the phase transition temperature, is shifted to lower regions. For irradiated crystals, the Curie temperature was $(44{\cdot}3 \pm 0{\cdot}5)$°C.

Crystals subjected to pre- or post-irradiation heat treatment at 95°C for about 100 hours have almost identical dielectric characteristics. Also, hysteresis measurements show, in the case of tempered crystals, an almost symmetrical double hysteresis loop. This may be due to the stabilization of domains during irradiation after annealing. The bias fields were 0·5 kV cm^{-1} for rejuvenated crystals and about 10 kV cm^{-1} for aged crystals. The crystals were annealed prior to each series of measurements in order to eliminate possible effects of ageing.

3.2. *ENDOR apparatus*

A superheterodyne spectrometer was used for all measurements [13]. It enables ENDOR measurements to be made over a range from 3 MHz to 70 MHz. Microwave power was approximately 0·2 mW at 77 K and 10 mW at 300 K; the nuclear resonance field strength was about 5 G.

The ENDOR resonance frequency was measured by means of calibration marks at intervals of 500 or 100 kHz. The error in the measurement was usually determined by the linewidth and was between 20 and 50 kHz. The cavity is a rectangular TE_{101} type where the sample is attached to one of the narrow sides. This arrangement was chosen to ensure good thermal contact of the sample with the external temperature bath. The ENDOR coil had one to five turns directly wound around the crystal. For measurements of the angular dependence of the ENDOR spectra only the field component perpendicular to the static magnetic field was used. Thus it was possible to monitor the angular variation over a range of $\pm 90°$ at 77 K and $\pm 25°$ at room temperature without reorienting the crystal.

Over the range from 20°C to 80°C a constant temperature at the sample was provided by the use of a constant-voltage heated oil bath in which the cavity, hermetically sealed by a metallic cap, was located. After thermal equilibrium was reached, the temperature was measured directly on the cavity using a thermocouple. The accuracy of measurement was approximately $\pm 0·5$°C.

For recording ENDOR spectra with an external electric d.c. field applied to the sample, a graphite electrode having a surface impedance of more than 1 MΩ had to be attached to the crystal facing the cavity wall and connected to the feeder cable through the use of highly conductive silver paste. The second electrode was insulated with a Teflon coat. This arrangement permits the attenuation of both microwave and radiofrequency fields to be held within acceptable limits; the loaded Q value of the cavity dropped to about 800. The arrangement allows measurements of anisotropy to be made about axes perpendicular to the crystallographic [010] axis over an angular range of $\pm 20°$. The dc fields thus obtained were in the order of 20 kV cm^{-1}.

4. Irradiation centres in TGS

Numerous E.P.R. studies made on TGS and glycine single crystals [12–14] have identified the following glycine radicals:

NH_3^+–CH–COO^- (type I)

$\dot{C}H_2$–COO^- (type II)

The type II radical is formed, from gly I, in the $y \approx \frac{1}{4}$ and $\frac{3}{4}$ planes. It has a lifetime of several weeks. This radical was not included in our studies. The

type I radical is formed, on gly II or gly III or at both of them, in the planes $y \approx \frac{1}{2}$ and 1.

Type I radicals with different motional characteristics of the amino group were detected at 77 K in the E.P.R. spectrum. For the majority of radicals at room temperature, the amino group was found to perform essentially free rotation about the CN bond. The temperature dependence of rotation is similar to that of the NH_3^+–$\dot{C}$H–COO^- radical observed by Reitböck [14, 15] in glycine single crystals. For glycine, rotation has been observed to decrease over the range $T < 126$ K so that the amino protons do not show equivalent behaviour.

ENDOR lines of protons of a rotating amino group were not observed at 77 K nor in the range from 290 K to 350 K. A rotational frequency of about 3×10^8 Hz may be concluded from the temperature dependence of E.P.R. spectra. Because of broadening effects this rotational frequency rules out the observation of ENDOR spectra.

All of the ENDOR studies described here were made on type-I radicals with strongly hindered rotation of the amino group. The concentration of these radicals at room temperature is about 20 times lower than that of radicals with fast rotation of the amino group. At 77 K and 300 K ENDOR spectra of these radicals showed the lines of one α-proton and three non-equivalent β-protons. The ENDOR spectra, shown in figure 1, consist of two sets of lines.

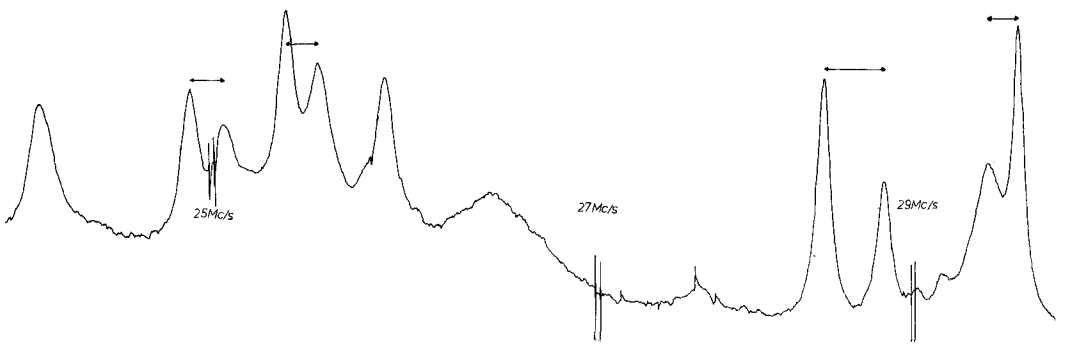

Figure 1. ENDOR spectrum of type-I radicals at gly II and gly III sites. **B** lies in the $(\bar{1}01)$ plane, the angle between **B** and [010] is 20°.

The angular dependences show an incorporation of the radicals at sites of gly II and gly III. The intensities of the lines do not depend on the distribution of domains in the crystal. The intensity ratio of the two sets of lines which is 1 : 1·4 can be attributed to a different electronic spin-lattice relaxation time (T_1) for radicals at the two sites of incorporation, with T_1 values being 70 μs for the radical at gly II and 40 μs for the radical at gly III. The T_1 values were determined by plotting the saturation curves of the ENDOR spectra.

5. Determination of the hamiltonian parameters

The ENDOR spectrum is described by the spin hamiltonian

$$\hat{H} = \mu_B \,.\, \mathbf{B} \,.\, \mathbf{g} \,.\, \mathbf{S} + \sum_{k=1}^{4} (\mathbf{S} \,.\, \mathbf{A} \,.\, \mathbf{I}_k - \mu_N \cdot g_{nk} \,.\, \mathbf{B} \,.\, \mathbf{I}_k), \qquad (1)$$

$$S = I_k = \tfrac{1}{2},$$

taking into account the Zeeman electron term and spin orbital coupling, as well as the Zeeman nuclear energy and hyperfine coupling of the α and the three β-protons. The interaction between nuclei is negligible. The principal values of the hyperfine tensors, which were determined by applying second-order perturbation theory to [1], are summarized in table 1 for a temperature of 25°C. They were determined in a coordinate system $\{x, y, z\}$ which corresponds to the system of the crystal axes $\{a, b, c^*\}$ with $c^* = c \sin \beta$. The accuracy was about ± 50 kHz (± 100 kHz for H_{11} and H_{16}) for the determination of the principal values and less than $\pm 5°$ for the directions of the principal tensor axes.

Table 1. Hyperfine coupling tensors of the radical at glycine II and glycine III sites at $T = 25$°C. l, m and n are the direction cosines to the axes x, y and z respectively.

	Results of ENDOR investigations					Calculated values	
Proton	A_0/MHz	A_{ii}/MHz	l	m	n	A_0/MHz	A_{ii}/MHz
		−16·45	0·2486	−0·1708	0·9534		−16·5
H_α(II)	−77·53	1·23	0·1073	0·9833	0·1474	−74·1	0·8
		15·14	−0·9626	0·0660	0·2629		15·6
		16·74	−0·7555	0·1302	0·6537		7·8
H_{12}	87·36	−0·84	0·1506	0·9571	−0·0206	88·2	1·0
		−15·80	0·6487	−0·0839	0·7564		−16·2
		15·31	−0·8489	−0·0911	0·5207		17·2
H_{10}	74·41	2·09	0·0831	−0·9961	−0·0251	79·2	1·1
		−17·91	0·5202	0·0317	0·8535		−20·2
		3·48	−0·0108	0·6994	−0·7147		4·6
H_{11}	2·05	2·10	0·1401	−0·7066	−0·6936	0·6	3·1
		−1·48	−0·9901	−0·1077	−0·0904		−7·7
		−16·05	0·2309	−0·1738	0·9573		—
H_α(III)	−77·26	1·42	0·0793	0·9840	0·1595	−75·0	—
		14·63	−0·9697	0·0392	0·2410		—
		16·76	−0·7578	0·1242	0·6406		—
H_{17}	87·52	−0·97	0·1282	0·9909	−0·4199	84·0	—
		−15·80	0·6401	−0·0486	0·7667		—
		15·31	−0·8340	−0·2395	0·4973		—
H_{15}	74·71	1·52	0·2638	−0·9639	−0·0258	81·0	—
		−16·83	0·4862	0·1066	0·8673		—
		3·63	0·0455	0·5633	0·3250		—
H_{16}	1·46	1·80	0·1992	−0·8145	−0·5450	4·0	—
		−2·51	−0·9789	−0·1340	−0·1494		—

6. Interpretation of experimental results

6.1. *INDO calculations*

To determine the radical structure by the INDO method, both the bond angles and bond lengths were varied. The testing parameters were the total energy, the spin densities characteristic of the π-electron radicals and the isotropic hyperfine constant A_0. The INDO calculations were carried out on

a CDC 1604A computer using the CN/INDO Fortran programme developed by Pople and Beveridge [16]. Since test calculations with spin annihilation lead only to a slight reduction of spin densities in the whole molecule, annihilation was abandoned to save computer time.

The isotropic hyperfine constant A_{0n} for nucleus n was calculated by assuming that only s-electrons of the nucleus considered have a probability density differing essentially from zero at the nuclear site. The following then applies:

$$A_{0n}=\frac{8\pi}{3} g_e\mu_B g_n\mu_N |\phi_{sn}(r_n)|^2 \rho_{sn} \tag{2}$$

where g_e and g_n are the g-factors for the electron and the nucleus n, respectively. ϕ_{sn} is the atomic orbital of the s-electron and ρ_{sn} the electron spin density, both at nucleus n. The components of the anisotropic hyperfine tensor were calculated from the π-electron spin density ρ_π. It was assumed that the electron spin density at carbon bonded to nitrogen (C_N) is restricted to the p_π-orbital and that the system is in a strong magnetic field. Thus the Hamiltonian for the anisotropic hyperfine tensor is

$$\hat{H}_d = -g_e g_n \mu_B \mu_N \hat{I}_z \hat{S}_z \sum_{\mu,\lambda} \langle\phi_\mu|\hat{T}|\phi_\lambda\rangle \rho_{\mu\lambda}, \tag{3}$$

with the first-order dipolar interaction operator $\hat{T}$

$$\hat{T} = |\mathbf{r}|^{-3} - 3z^2|\mathbf{r}|^{-5} \tag{4}$$

and with $\mathbf{r}$ the vector from the relevant proton to the electron in the p_π-orbital at the C_N atom, ϕ_μ, ϕ_λ the π and s-orbital at C_N and $\rho_{\mu\lambda}$ the elements of the spin-density matrix

To calculate the matrix elements $\langle\phi_\mu|\hat{T}|\phi_\lambda\rangle$ for protons outside the nodal plane of the π-orbital we used Derbyshire's relation [17] for the dipole–dipole interaction.

For the hyperfine splitting of the β-protons a further essential contribution due to spin polarization and hyperconjugation [18] was taken into account.

6.2. *Results and discussion of the INDO calculations*

From the ENDOR experiments it was not possible to obtain the angle φ between the plane of the COO^- group and that of CC_NN. For $\varphi=90°$ a distinct minimum of the total energy appears which is about 126 kJ/mol lower than the total energy for $\varphi=0°$. This structure is confirmed by the spin density in the p_π-orbital which increases from 0·3 for $\varphi=0°$ to 0·8 for $\varphi=90°$, thus reaching values typical of π-electron radicals. Following this structural change are marked shifts of spin density in the molecule, and hence of the isotropic hyperfine constant. The bond lengths $\overline{C_NN}$, $\overline{C_NH_\alpha}$ and the three $\overline{NH_\beta}$ are in agreement with the results of structure investigations [11].

Taking account of the fact that both the symmetry of the radical and sp^2-hybridization at the C_N atom are consistent with theoretical molecular models, the position of the α-proton was determined. The α-proton is displaced from the $\overline{CC_NN}$ plane by an angle $\theta=10°$. The results are summarized in table 2.

The results of the INDO calculations demonstrate that the radical structure deviates from that of the glycine molecules in the undisturbed crystal. CNDO

Table 2. Bond lengths and bond angles of radicals of type I at sites glycine II and III in comparison to those of the undamaged glycine molecules given by Hoshino *et al.* [9]. Hydrogen bond lengths were taken from Itoh *et al.* [10].

	Radical at glycine II			Radical at glycine III	
	INDO calculations	Hoshino *et al.* [9]		INDO calculations	Hoshino *et al.* [9]
$\overline{C_NN}$/Å	1·45	1·50	$\overline{C_NN}$/Å	1·40	1·45
$\overline{C_NC}$/Å	1·50	1·55	$\overline{C_NC}$/Å	1·50	1·51
$\overline{CO}$/Å	1·25	1·23	$\overline{CO}$/Å	1·25	1·25
$\overline{CO'}$/Å	1·30	1·29	$\overline{CO'}$/Å	1·30	1·31
$\overline{C_NH_\alpha}$/Å	1·25	1·20	$\overline{C_NH_\alpha}$/Å	1·25	1·20
$\overline{NH_{12}}$/Å	1·05	1·23	$\overline{NH_{17}}$/Å	1·05	0·95
$\overline{NH_{10}}$/Å	1·05	1·02	$\overline{NH_{15}}$/Å	1·05	0·92
$\overline{NH_{11}}$/Å	1·00	0·98	$\overline{NH_{16}}$/Å	1·00	0·88
$\overline{C_NH_{12}}$/Å	2·02	2·27	$\overline{C_NH_{17}}$/Å	1·94	2·00
$\overline{C_NH_{10}}$/Å	1·99	2·15	$\overline{C_NH_{15}}$/Å	1·96	1·91
$\overline{C_NH_{11}}$/Å	2·00	2·04	$\overline{C_NH_{16}}$/Å	1·90	1·98
$\overline{CC_NN}$; $\overline{COO'}$	90°	20°	$\overline{CC_NN}$; $\overline{COO'}$	90°	0°
$\overline{CC_NN}$; $\overline{C_NH_\alpha}$	10°	—	$\overline{CC_NN}$; $\overline{C_NH_\alpha}$	10°	—
$\overline{CC_N}$; $\overline{C_NN}$	109°	107°	$\overline{CC_N}$; $\overline{C_NN}$	109°	110°

calculations, performed by Oegerle and Sabin [19] for glycine, gave similar results with regard to the molecular energy, orbital energies and dipole moments, but they found an essentially smaller deviation from the planar structure ($\varphi = 20°$). This may be a consequence of a greatly changed bonding structure at the C_N atom due to the removal of a proton from the glycine molecule. Our investigations indicate a marked dependence of s-electron spin density on the relative position of the C_NH_α bond to the p_π-orbital.

In spite of the approximation procedures used to calculate the coupling constants and the inaccuracies inherent in spin-density calculations, the hyperfine parameters are in good agreement with the experimental ENDOR results. Improvements should be possible particularly as regards the anisotropic values for the β protons when the influence of the surrounding groups of the lattice on radical structure is taken into account.

6.3. *The positions of radicals in the crystal lattice and refinements of radical structure*

Our theoretical studies were made on isolated glycine radicals, because the limits of the computer prohibited making allowance for the interaction of the radicals with the crystal lattice. However, in the lattice the COO^- group is bonded to a further glycine ion by a hydrogen bridge and the NH_3 group is bonded to SO_4^{2-} groups. The total energy for rotation of the NH_3 group about the C_NN bond, shows a minimum of about 4·2 kJ/mol for an angle θ_m [17]

of about 40°; $\theta_m(17)$ denotes the angle between the plane $\overline{C_N NH_{17}}$ and the plane formed by the p_π-orbital and the $C_N N$ bond. This energy variation is of the same order of magnitude as the hydrogen bridge bonding energy. Therefore we estimated the angle θ_m which is important for the description of ferroelectric structural changes using McLachlan's [20] empirical formula,

$$A_0 = \rho_\pi (B_0 + B_1 \cos^2 \theta_m). \tag{5}$$

When we take the bond length $\overline{C_N H_\alpha} = 1{\cdot}24$ Å, the calculated spin density $\rho_\pi = 0{\cdot}87$, the directions of the p_π-orbital measured by E.P.R. and that of the $C_N H_\alpha$ bond of glycine III determined by ENDOR an inclination of the p_π-orbital of 9° and of the $C_N H_\alpha$ bond of $-2°$ relative to the plane of the undisturbed molecule is obtained. This result is in good agreement with the angle of 10° between the $C_N H_\alpha$ direction and the p_π-orbital, as obtained from INDO calculations. From the experimental values of the hyperfine interaction of the β-protons we find

$$B_0 = \quad 1{\cdot}66 \text{ MHz},$$
$$B_1 = 121{\cdot}6 \text{ MHz},$$

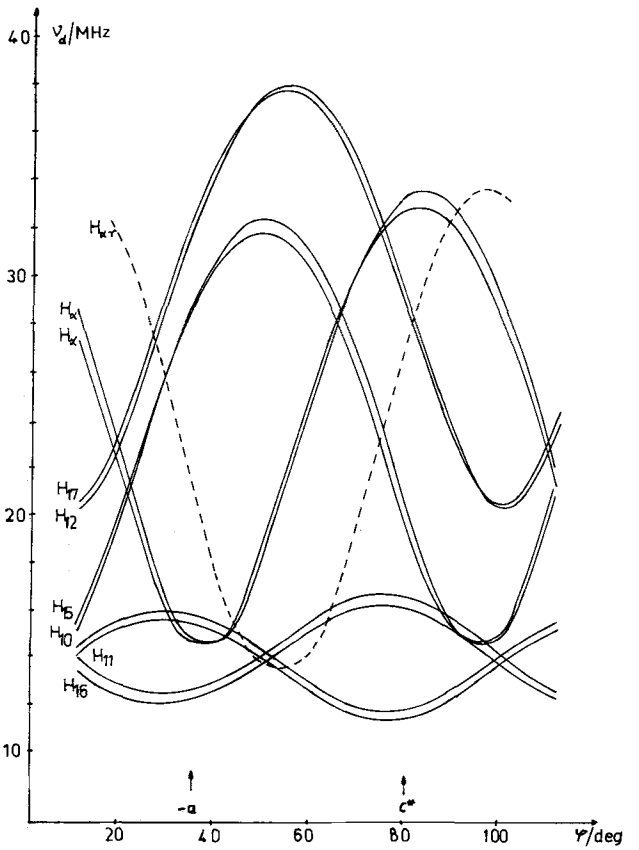

Figure 2. Angular variation of the ENDOR spectra measured at 77 K. **B** rotates in the (010) plane. The dashed curve shows the angular variation of the α-proton hyperfine coupling at 300 K.

and $\theta_m = 25{\cdot}4°$ for the proton H_{17}. Comparison with the INDO calculation suggests a deformation of the radical caused by the hydrogen bridges between the radical and the lattice.

Kato and Abe [11] have shown that the radicals at gly II and gly III have freely rotating amino groups and almost a planar structure. The trigonal bond angle, $\widehat{NC_NC}$ is approximately 123°. There is good agreement between the bond directions C_NN and C_NC and the corresponding directions determined by the X-ray structure [9] and deuteron magnetic resonance investigations [1, 2].

For the radicals with strongly hindered rotation of the amino group, which are dealt with in this paper, a substantial difference was observed between angular dependence on the hyperfine structure for the α-protons and that found at 300 K using E.P.R.

In figure 2 the angular dependence of ENDOR spectra at 77 K for radicals with an extremely slowly rotating group is compared with the E.P.R. angular dependence for the α-proton measured at 300 K. Both the angular dependence of the E.P.R. spectra at 300 K for the radical with a rotating amino group, and that of the ENDOR spectra at 77 K for an extremely slowly rotating group are compared in figure 2. The spectra clearly show a reorientation of the tensor main axis in the (010) plane. If it is assumed that the C_NH_α bond is symmetric with C_NN and C_NC, then one must consider a reorientation of the radical, by approximately 29° about an axis which passes through C_N and is normal to the plane of the radical.

Careful E.P.R. studies made at 77 K show that at this temperature there also exist two sets of spectra corresponding to type-I radicals in different rotational states and with different tensor axis directions for the α-proton. Both spectra at 77 K are shown in figure 3 in comparison with the stick spectra constructed from E.P.R. data for 300 K (rotating amino group) and from ENDOR data for

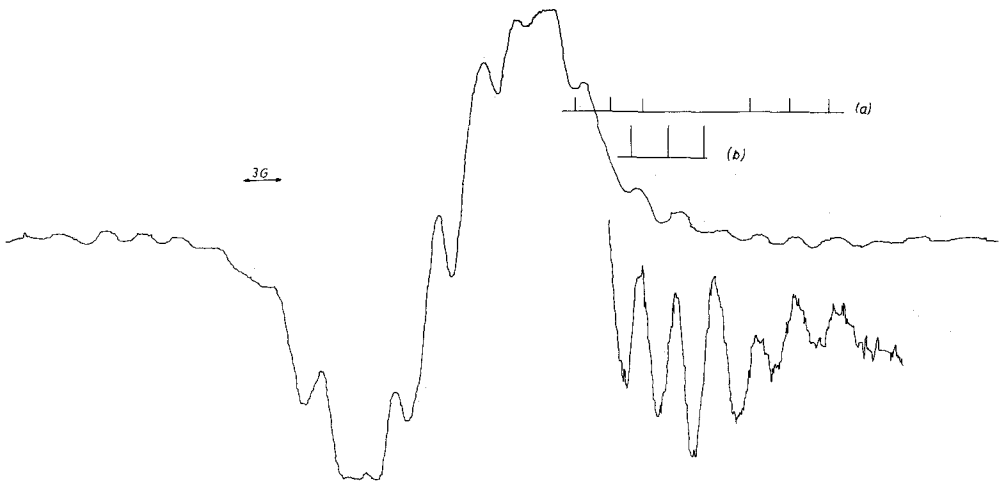

Figure 3. E.P.R. spectrum at 77 K. Stick diagram for comparison. (*a*) For a rotating NH_3 group from E.P.R. data at 300 K and (*b*) for a strongly restricted NH_3 group from ENDOR data at 77 K.

77 K (restricted rotation of amino group and tilted α-tensor axes). It demonstrates that the reorientation of the α-tensor axes is obviously related to a slowing of the rotation of the amino group. The assumption of both rotation and internal twist also gives good agreement for the β-proton positions determined by the INDO calculation (see table 2) and following from equation (5) with the positions of the hydrogen bridges in the crystal (see figure 4). The hydrogen bridge system of the NH_3 group is not changed by irradiation.

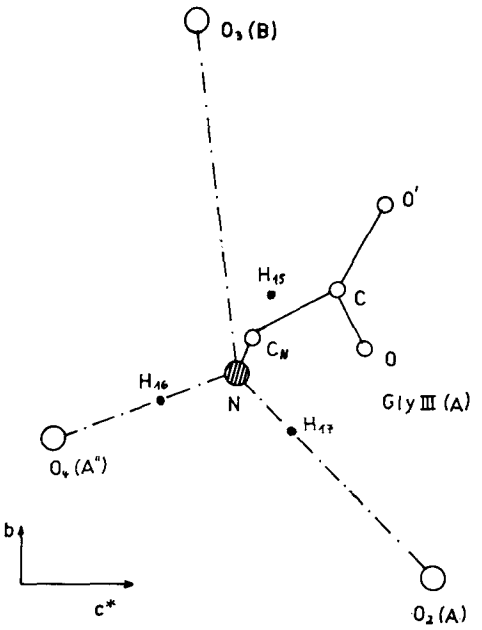

Figure 4. Positions of hydrogen atoms of the gly III radical and the corresponding hydrogen bonds N–H . . . O of the undamaged molecule, after Hoshino *et al.* [9].

The measured parameters, especially the high value for the isotropic hyperfine constant for the α-proton, are in agreement with an angle $\widehat{NC_NC}$ of 109° and an inclination of the C_NH_α bond with respect to the p_π-orbital of 9°.

The structural parameters derived will be the starting-point for a discussion of the structural differences between radicals at gly II and gly III sites and of the temperature dependence of these differences in the ferroelectric phase of TGS, which will be conducted in part 2.

This research has been performed in the Arbeitsgruppe E.P.R. an Festkörpern, Sektion Physik, Karl-Marx-Universität Leipzig. The valuable help and assistance received from numerous colleagues have been appreciated.

References

[1] Blinc, R., Pintar, M., and Župančič, I., 1967, *J. Phys. Chem. Solids*, **28**, 405.
[2] Bjorkstam, J. L., 1967, *Phys. Rev.*, **153**, 599.
[3] Blink, R., Osredkar, R., Prelesnik, A., and Župančič, I., 1971, *J. chem. Phys.*, **55**, 4843.

[4] OVENALL, D. W., and MÜLLER, K. A., 1961, *Helv. phys. Acta*, **34,** 786.
[5] BLINC, R., DETONI, S., LEVSTEK, I., PINTAR, M., POBERAJ, S., and SCHARA, M., 1961, *J. Phys. Chem. Solids*, **20,** 187.
[6] SCHULGA, Z. S., 1968, *Ukr. fiz. Zh.*, **13,** 211.
[7] KATO, I., and ABE, R., 1973, *J. phys. Soc. Japan*, **32,** 717.
[8] KATO, I., and ABE, R., 1969, *J. phys. Soc. Japan*, **26,** 948.
[9] HOSHINO, S., OKAYA, Y., and PEPINSKY, R., 1959, *Phys. Rev.*, **115,** 323.
[10] ITOH, K., and MITSUI, I., 1971, *Ferroelectrics*, **2,** 255.
[11] KAY, M. I., and KLEINBERG, R., 1973, *Ferroelectrics*, **5,** 45.
[12] NITSCHE, R., 1958, *Helv. phys. Acta*, **31,** 306.
[13] WELTER, M., and HEINHOLD, D., 1978, *Exp. Tech. Phys.* (in the press).
[14] REITBÖCK, H., 1969, *Z. Naturf.* A, **24,** 271.
[15] REITBÖCK, H., 1969, *Biophysik*, **4,** 15.
[16] POPLE, J. A., and BEVERIDGE, L. D., 1970, *Approximate Molecular Orbital Theory* (McGraw-Hill Book Company).
[17] DERBYSHIRE, W., 1962, *Molec. Phys.*, **5,** 225.
[18] MCCONNELL, H. M., and STRATHDEE, J., 1959, *Molec. Phys.*, **2,** 129.
[19] OEGERLE, W. R., and SABIN, J. R., 1973, *J. molec. Struct.*, **15,** 1316.
[20] MCLACHLAN, A. D., 1958, *Molec. Phys.*, **1,** 233.